Electronic Supplementary Information

for

Sterically geared tris-thioureas; transmembrane chloride transporters with unusual activity and accessibility

Hennie Valkenier, Christopher M. Dias, Kathryn L. Porter Goff, Ondřej Jurček, Rakesh Puttreddy, Kari Rissanen, Anthony P. Davis

Contents

1. Synthesis

General Synthetic Experimental Information.

All commercially available compounds were used without further purification. THF was dried by passing through a modified Grubbs system[1] with an alumina column. Anhydrous DMF was purchased from Alfa Aesar. All reactions were performed under N_2. Flash column chromatography was performed using silica gel (Aldrich, pore size 60 Å, particle size 40-63 µm) as the absorbent. Routine monitoring of reactions was performed using precoated silica gel TLC plates (Merck silica gel 60 F_{254}). Spots were visualised by UV light.

^{1}H and ^{13}C NMR spectra were recorded using ECS 400, Varian 400, Varian 500a (carbon sensitive), Varian 500b (proton sensitive), or Bruker Ascend 500 MHz cryoprobe (carbon sensitive) spectrometers. All chemical shifts (δ) are quoted in parts per million (ppm) and the residual solvent signal was used to reference the spectrum. Signal splittings are described as singlet (s), doublet (d), triplet (t), quartet (q), septet (sept), and multiplet peaks (m).

Mass spectra by electrospray ionisation (positive mode) were recorded on a Bruker MicrOTOF. Infrared spectra were recorded on a Perkin Elmer Spectrum Two FT-IR. Elemental analysis was carried out by the Microanalysis Department at the School of Chemistry, University of Bristol.

The carbon numbering system for **6** is outlined below:

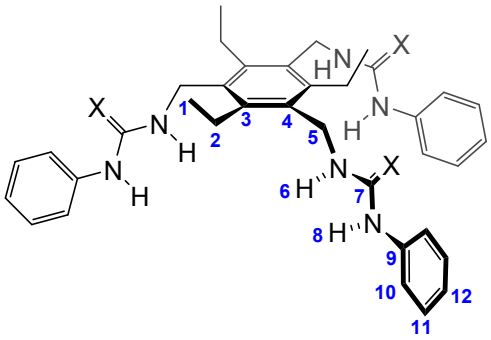

Synthesis of 1,3,5-tris(phenylthioureidomethyl)-2,4,6-triethylbenzene, **6SP**

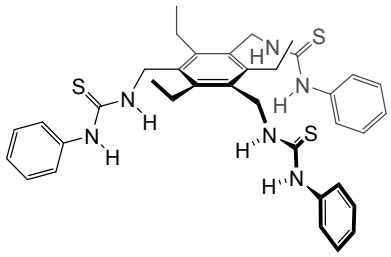

To a mixture of 2,4,6-triethyl-1,3,5-benzenetrimethanamine **5** (50 mg, 200 µmol) and phenyl isothiocyanate (79 µL, 662 µmol, 3.3 eqv.) was added anhydrous THF (5 mL) and the resulting white suspension stirred at room temperature for 18 h. The mixture was concentrated *in vacuo* to give a white solid which was purified by flash column chromatography over silica gel eluted with 0.5-10% methanol in dichloromethane to give **6SP** as a white solid (81 mg, 124 µmol, 62%). R_f = 0.20 (10% MeOH in DCM); ^{1}H NMR (400 MHz, acetone-d_6) δ 8.96 (s, 3H, *NH8*), 7.57 – 7.50 (m, 6H, *H10*), 7.35 – 7.28 (m, 6H, *H11*), 7.16 – 7.09 (m, 3H, *H12*), 6.83 (s, 3H, *NH6*), 4.81 (d, *J* = 4.1 Hz, 6H, *H5*), 2.81 (q, *J* = 7.6 Hz, 6H, *H2*), 1.18 (t, *J* = 7.5 Hz, 9H, *H1*); ^{13}C NMR (126 MHz, acetone-d_6) δ 181.8 (*C7*), 145.4 (*C3*), 140.1 (*C9*), 133.0 (*C4*), 129.7 (*C11*), 125.6 (*C12*), 124.3 (*C10*), 43.9 (*C5*), 23.8 (*C2*), 16.9 (*C1*); IR (neat) $\bar{\nu}$/cm^{-1} 3398, 3164, 3001, 2969, 1591, 1529, 1508, 1493, 1293; HRMS (ESI): *m/z* calculated for $C_{36}H_{42}N_6NaS_3$ $[M+Na]^+$ 677.2525, found 677.2523.

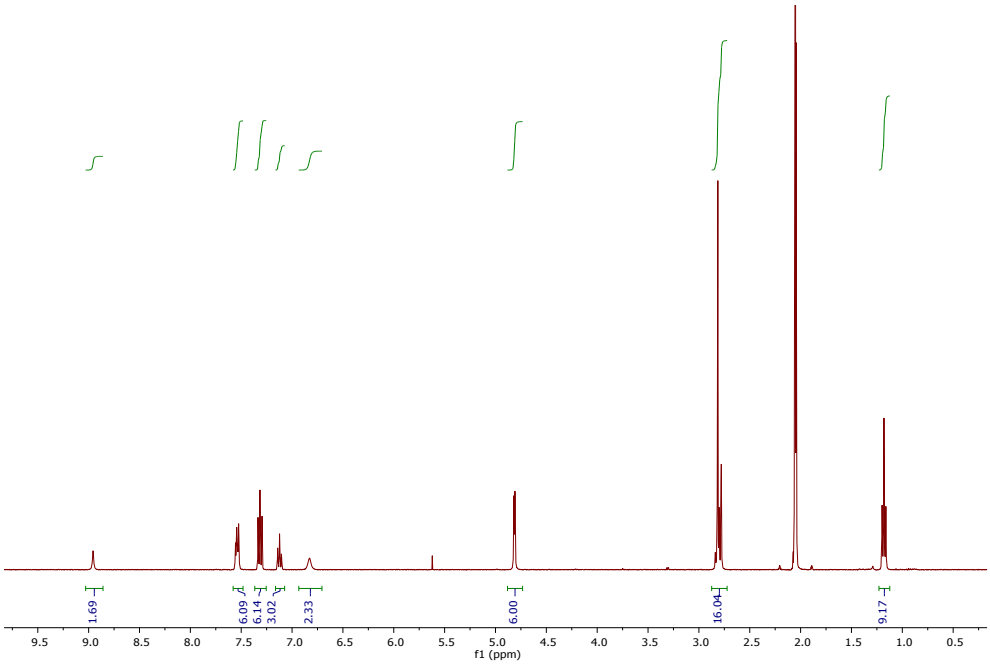

Figure S1. ^{1}H NMR spectrum of **6SP** in acetone-d_6.

Synthesis of 1,3,5-tris(4-nitrophenylthioureidomethyl)-2,4,6-triethylbenzene, **6SN**

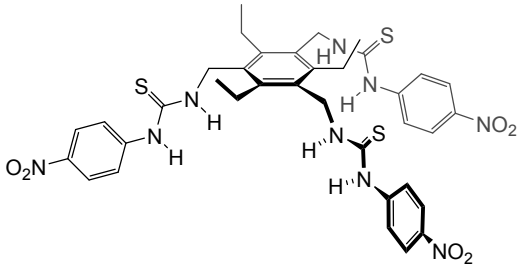

2,4,6-Triethyl-1,3,5-benzenetrimethanamine **5** (50.3 mg, 201 µmol) and 4-nitrophenyl isothiocyanate (120 mg, 666 µmol, 3.3 eqv.) were placed in 10 mL round bottom flask. Anhydrous THF (10 mL) was added and the reaction mixture was stirred at room temperature for 21 h. The crude material was concentrated and purified by column chromatography over silica gel eluted with 5% methanol in dichloromethane to give **6SN** as a yellow solid (140 mg, 177 µmol, 88%). R_f = 0.27 (5% MeOH in DCM); ^{1}H NMR (500 MHz, DMSO-d_6) δ 10.11 (s, 3H, *NH8*), 8.18 (d, *J* = 9.3 Hz, 6H, *H11*), 8.11 (s, 3H, *NH6*), 7.96 (d, *J* = 9.2 Hz, 6H, *H10*), 4.75 (d, *J* = 4.1 Hz, 6H, *H5*), 2.76 (q, *J* = 7.4 Hz, 6H, *H2*), 1.18 (t, *J* = 7.4 Hz, 9H, *H1*); ^{13}C NMR (126 MHz, DMSO-d_6) δ 179.3 (*C7*), 146.3 (*C12*), 144.3 (*C3*), 141.9 (*C9*), 131.7 (*C4*), 124.5 (*C11*), 120.2 (*C10*), 42.2 (*C5*), 23.0 (*C2*), 16.4 (*C1*); IR (neat) $\bar{\nu}$/cm^{-1} 3368, 3318, 2971, 1598, 1574, 1509, 1496, 1427, 1296, 1247, 1216, 1177, 1113, 852, 756; HRMS (ESI): *m/z* calculated for $C_{36}H_{39}N_9NaO_6S_3^+$ [M+Na]$^+$: 812.2078, found 812.2085.

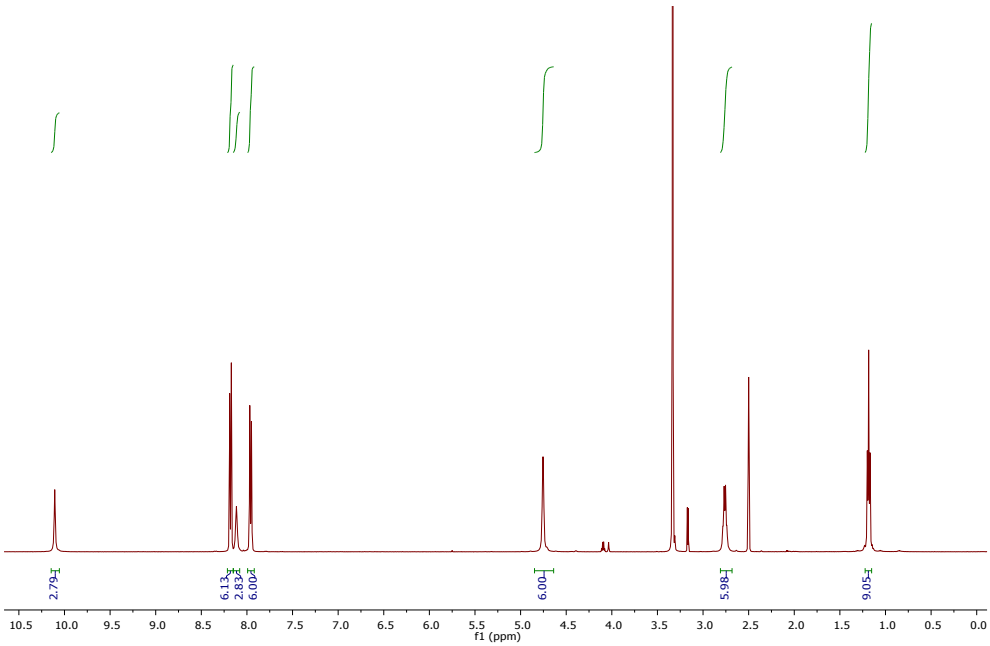

Figure S2. ^{1}H NMR spectrum of **6SN** in DMSO-d_6.

Synthesis of 1,3,5-tris(4-(trifluoromethyl)phenylthioureidomethyl)-2,4,6-triethylbenzene, **6SF**

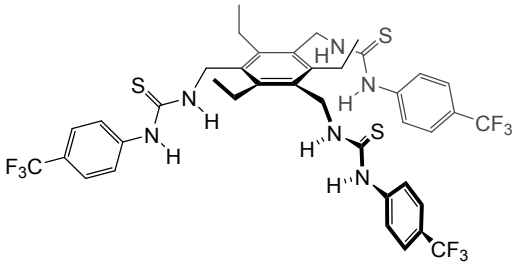

4-(Trifluoromethyl)phenyl isothiocyanate (167 mg, 0.82 mmol, 4.2 eqv.) was added dropwise to a solution of 2,4,6-triethyl-1,3,5-benzenetrimethanamine **5** (48.6 mg, 195 µmol) in anhydrous DMF (0.5 mL) and the resulting solution was stirred at room temperature for 21 h. The reaction mixture was concentrated under reduced pressure and residual DMF was removed through co-evaporation with toluene (3 x 20 mL). The crude material obtained was purified by flash column chromatography over silica gel eluted with 40-70% ethyl acetate in hexane to give **6SF** as a cream solid (90 mg, 105 µmol, 54%). R_f = 0.46 (6% MeOH in DCM); ^{1}H NMR (500 MHz, acetone-d_6) δ 9.16 (s, 3H, *NH8*), 7.89 (d, *J* = 8.5 Hz, 6H, *H10*), 7.64 (d, *J* = 8.5 Hz, *H11*), 7.23 (s, 3H, *NH6*), 4.87 (d, 6H, *J* = 4.3 Hz, *H5*), 2.86 (q, *J* = 7.5 Hz, 6H, *H2*), 1.23 (t, *J* = 7.5 Hz, 9H, *H1*); ^{13}C NMR (126 MHz, acetone-d_6) δ: 181.5 (*C7*), 145.6 (*C3*), 144.4 (*C9*), 133.0 (*C4*), 126.5 (q, *J* = 3.9 Hz, *C11*), 125.7 (q, *J* = 32.3 Hz, *C12*), 125.4 (q, *J* = 270.9 Hz, *CF$_3$*), 122.9 (*C10*), 43.7 (*C5*), 23.9 (*C2*), 16.8 (*C1*); ^{19}F NMR (470 MHz, acetone-d_6) δ: -62.45; IR (neat) $\bar{\nu}$/cm^{-1} 3230, 2969, 1615, 1516, 1321, 1243, 1163, 1108, 1065, 1015, 838; HRMS (ESI): *m/z* calculated for $C_{39}H_{39}F_9N_6NaS_3^+$ $[M+Na]^+$: 881.2147, found 881.2152; Elemental analysis: % calculated for $C_{39}H_{39}F_9N_6S_3$: C 54.53, H 4.59, N 9.79, found: C 54.49, H 4.82, N 9.64.

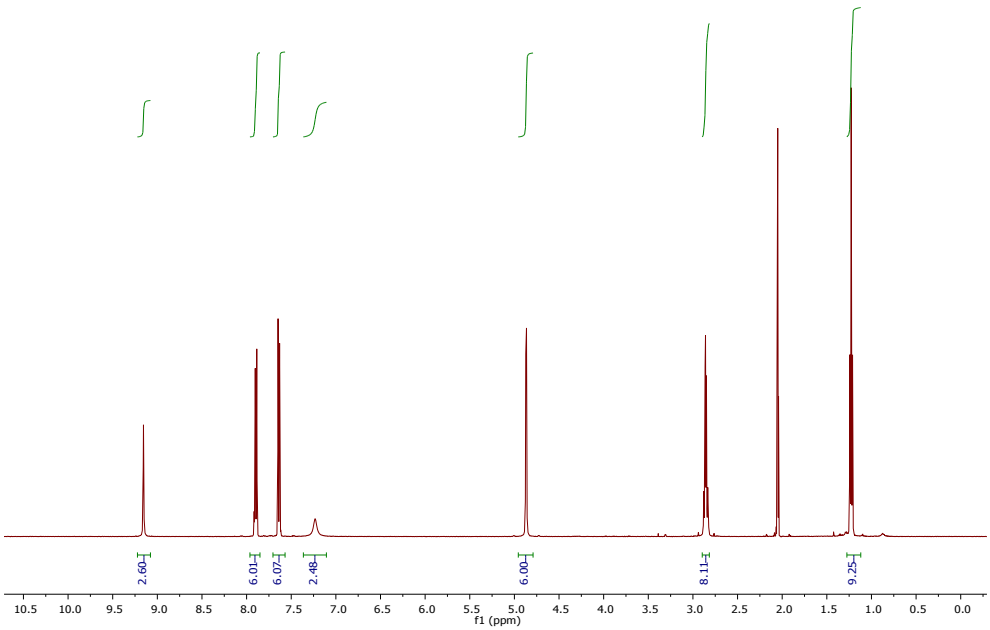

Figure S3. ^{1}H NMR spectrum of **6SF** in acetone-d_6.

Synthesis of 1,3,5-tris(3,5-bis(trifluoromethyl)phenylthioureidomethyl)-2,4,6-triethylbenzene, **6SF2**

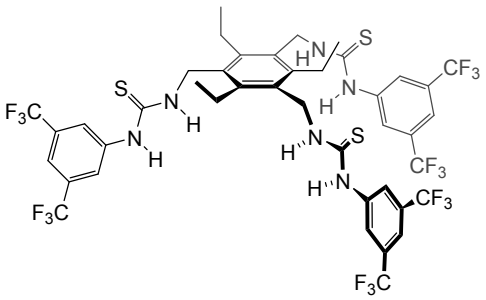

2,4,6-triethyl-1,3,5-benzenetrimethanamine **5** (68 mg, 273 µmol) was placed in a 25 mL round bottom flask and suspended in anhydrous THF (12 mL). 3,5-bis(trifluoromethyl)phenyl isothiocyanate (165 µL, 904 µmol, 3.3 eqv.) was added to the suspension and the reaction mixture was stirred at room temperature for 23 h. The crude material was concentrated and purified by flash column chromatography over silica gel eluted with 3% methanol in dichloromethane to give **6SF2** as an off-white solid (161 mg, 152 µmol, 56%). R_f = 0.31 (6% MeOH in DCM); ^{1}H NMR (400 MHz, acetone-d_6) δ: 9.34 (s, 3H, *NH8*), 8.38 (s, 6H, *H10*), 7.72 (s, 3H, *H12*), 7.48 (s, 3H, *NH6*), 4.89 (d, *J* = 3.9 Hz, 6H, *H5*), 2.87 (q, *J* = 7.2 Hz, 6H, *H2*), 1.25 (t, *J* = 7.4 Hz, 9H, *H1*); ^{13}C NMR (126 MHz, acetone-d_6) δ 181.6 (*C7*), 145.8 (*C3*), 142.9 (*C9*), 132.8 (*C4*), 131.9 (q, *J* = 33.2 Hz, *C11*), 124.4 (q, *J* = 272.0 Hz, *CF$_3$*), 123.1 (*C10*), 117.5 (*C12*), 43.8 (*C5*), 24.0 (*C2*), 16.8 (*C1*); ^{19}F NMR (470 MHz, acetone-d_6) δ: -63.55; IR (neat) $\tilde{\nu}$/cm^{-1} 3244, 2971, 1516, 1470, 1380, 1275, 1171, 1127, 949, 885, 701, 681; HRMS (ESI): *m/z* calculated for $C_{42}H_{36}F_{18}N_6NaS_3$ $[M+Na]^+$ 1085.1774, found 1085.1758.

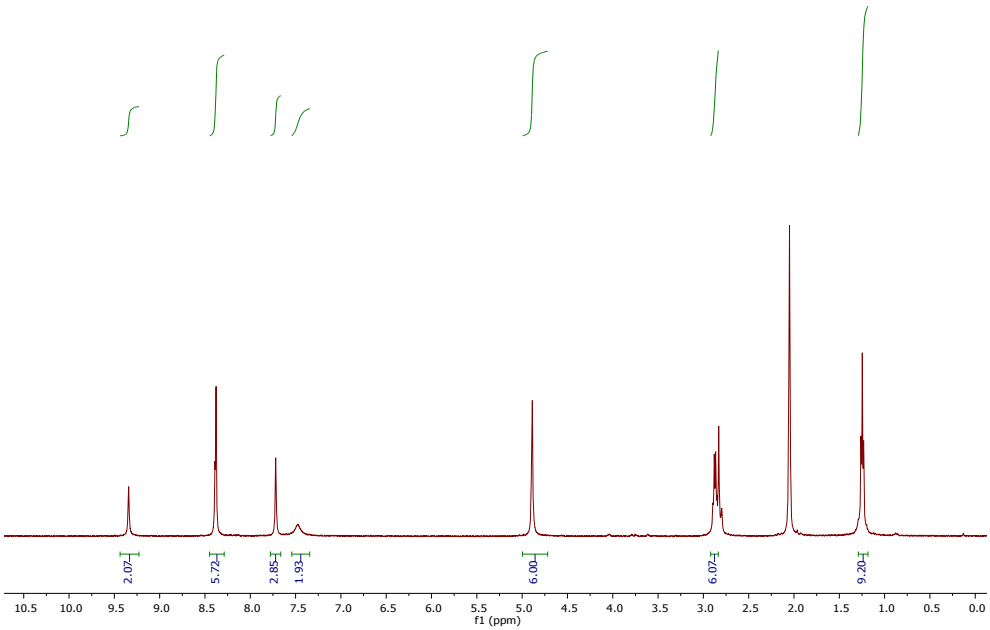

Figure S4. ^{1}H NMR spectrum of **6SF2** in acetone-d$_6$.

Synthesis of 1,3,5-tris(3,5-bis(trifluoromethyl)phenylureidomethyl)-2,4,6-triethylbenzene, **6OF2**

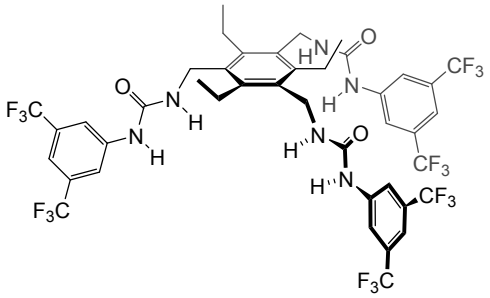

To a mixture of 2,4,6-triethyl-1,3,5-benzenetrimethanamine **5** (50 mg, 200 µmol) and 3,5-bis(trifluoromethyl)phenyl isocyanate (114 µL, 662 µmol, 3.3 eqv.) was added anhydrous DMF (2 mL) and the solution stirred at room temperature for 72 h. The solvent was removed by co-evaporation with toluene (5 x 5 mL) to give a yellow solid which was purified by flash column chromatography over silica gel eluted with a gradient of 1% methanol in dichloromethane to 2% methanol in ethyl acetate to give **6OF2** as a white solid (66 mg, 65 µmol, 32%). R_f = 0.44 (EtOAc-hexane 2:3); ^{1}H NMR (400 MHz, acetone-d_6) δ 8.47 (s, 3H, *NH8*), 8.16 – 8.11 (m, 6H, *H10*), 7.56 – 7.53 (m, 3H, *H12*), 6.05 (s, 3H, *NH6*), 4.54 (d, *J* = 4.8 Hz, 6H, *H5*), 2.91 (q, *J* = 7.5 Hz, 6H, *H2*), 1.23 (t, *J* = 7.4 Hz, 9H, *H1*); ^{13}C NMR (126 MHz, acetone-d_6) δ 155.2 (*C7*), 144.6 (*C3*), 143.5 (*C9*), 133.8 (*C4*), 132.4 (q, *J* = 32.9 Hz, *C11*), 124.5 (q, *J* = 271.9 Hz, *CF$_3$*), 118.4 (*C10*), 114.9 (sep., *J* = 3.8 Hz, *C12*), 38.8 (*C5*), 23.5 (*C2*), 16.9 (*C1*); ^{19}F NMR (377 MHz, acetone-d_6) δ -63.56 (*CF$_3$*); IR (neat) $\tilde{\nu}$/cm^{-1} 3320 (br m, N–H), 2972 (w, C–H), 2937 (w, C–H), 1640 (s), 1557 (s), 1471 (m), 1384 (s), 1274 (s), 1120 (s); HRMS (ESI): *m/z* calcd for $C_{42}H_{36}F_{18}N_6NaO_3$ $[M+Na]^+$ 1037.2454, found 1037.2457.

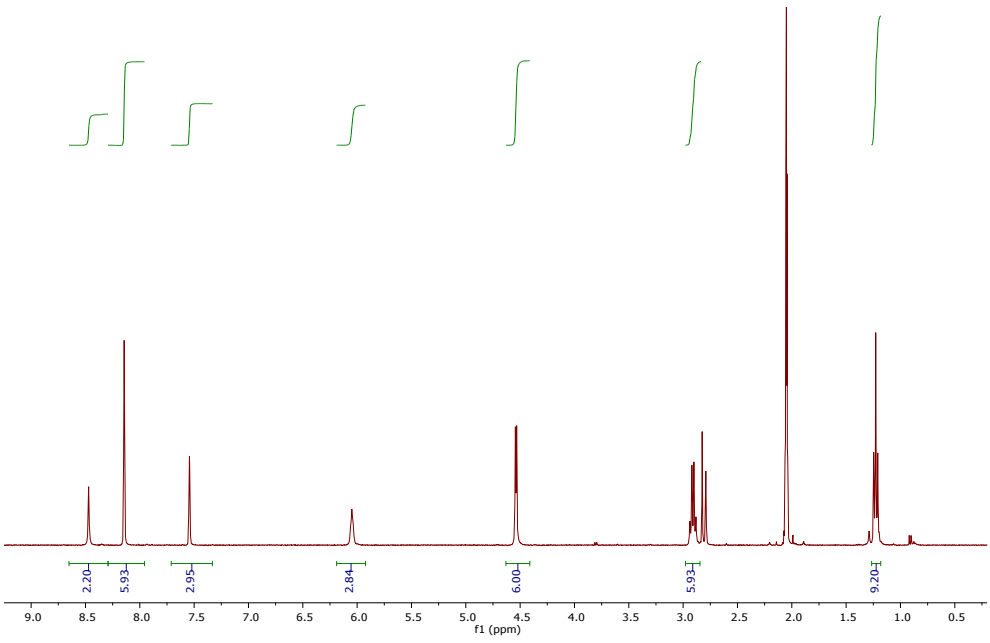

Figure S5. ^{1}H NMR spectrum of **6OF2** in acetone-d$_6$.

2. Binding studies

Measurement of affinities to $Et_4N^+Cl^-$ in chloroform through extraction from water

This method is adapted from Clare *et al.*[2] The $Et_4N^+Cl^-$ salt was obtained from Sigma Aldrich and dried under vacuum overnight prior to solution preparation using deionised water that had been passed through a Millipore filtration system. All host solutions were prepared using chloroform that had been deacidified by passage through a flash chromatography column containing basic alumina.

A solution of host in deacidified chloroform was combined with 10 mL of aqueous $Et_4N^+Cl^-$ guest solution in a sample tube (30 mL). Concentrations and volumes are specified in Table S1. A magnetic stirring bar (2 cm) was added to the tube and the lower half was immersed in a water bath heated to 303 K, while the contents were stirred vigorously to achieve good mixing of the two phases. After 30 minutes, stirring was stopped and the two phases were allowed to separate. The majority of the aqueous phase was then removed using a pipette and the remaining organic phase was centrifuged for 10 minutes at 4000 rpm. The chloroform solution was then filtered through Whatman 1PS hydrophobic filter paper to remove any remaining aqueous phase. Solvent from the filtrate was then removed *in vacuo* and the solid was further dried under vacuum. The resulting solids from the extraction experiments were dissolved in acetone-d_6 and the solutions were analysed with ^{1}H NMR spectroscopy.

A value for the molar ratio (R) was determined by integrating the signal at $\delta = 3.5$ ppm ($C\underline{H}_2$ of $Et_4N^+Cl^-$) against the $C\underline{H}_2NH$ signals for **6** (~ 4.8 ppm) and the aryl CH of **4SF** (7.6 ppm). This process was repeated for different concentrations of the salt solution.

The values for R obtained from the ^{1}H NMR spectra were used to calculate values for the equilibrium extraction constants K_e:

$$H_{org} + X^-_{aq} + Y^+_{aq} \overset{K_e}{\rightleftharpoons} HX^-Y^+_{org} \qquad K_e = \frac{[HX^-Y^+]_{org}}{[H]_{org}[X^-]_{aq}[Y^+]_{aq}}$$

$$K_e = \frac{R}{(1-R)\left([G]^{initial}_{aq} - R\frac{V_{org}}{V_{aq}}[H]^{initial}_{org}\right)^2}$$

To convert the extraction constants K_e into association constants K_a it is necessary to obtain the distribution constants K_d for the substrates between aqueous and organic phases:

$$X^-_{aq} + Y^+_{aq} \overset{K_d}{\rightleftharpoons} X^-Y^+_{org} \qquad K_d = \frac{[X^-Y^+]_{org}}{[X^-]_{aq}[Y^+]_{aq}}$$

The K_d value for tetraethylammonium chloride partitioning between water and chloroform has been determined and reported previously to be 1.269×10^{-5} M^{-1}.[3]

The binding constant K_a is then calculated from K_e and K_d :

$$H_{org} + X^- Y^+_{org} \overset{K_a}{\rightleftharpoons} HX^- Y^+_{org} \qquad K_a = \frac{[HXY]_{org}}{[H]_{org}[X^- Y^+]_{org}} = \frac{K_e}{K_d}$$

When [G] > 50 mM, the amount of salt that migrates from the aqueous phase into the organic phase without assistance of the host has to be taken into account by correcting the measured value of R as follows:

$$R = R_{measured} - \frac{K_d \left([G]^{initial}_{aq}\right)^2}{[H]^{initial}_{org}}$$

Table S1. Overview of the conditions and results from the extraction experiments

Receptor	[H] (mM)	[G] (mM)	V_{org} (mL)	V_{aq} (mL)	$R_{measured}$	K_a (M^{-1})
6SP	0.10	1300	8.0	10.0	0.504	1.9×10^4
	0.10	1400	8.0	10.0	0.553	1.8×10^4
	0.10	1500	8.0	10.0	0.635	1.9×10^4
					Average:	**1.9×10^4**
6SF	0.080	75	9.0	10.0	0.469	1.2×10^7
	0.080	100	9.0	10.0	0.563	1.0×10^7
	0.080	150	9.0	10.0	0.865	2.2×10^7
					Average:	**1.5×10^7**
6SF2	0.29	10	3.0	10.0	0.479	7.3×10^8
	0.29	15	3.0	10.0	0.653	6.6×10^8
	0.28	25	3.0	10.0	0.834	6.4×10^8
					Average:	**6.8×10^8**
4SF *	0.10	400	7.0	10.0	0.423	3.3×10^5
	0.10	500	8.0	10.0	0.480	2.6×10^5
	0.10	600	8.0	10.0	0.594	2.7×10^5
					Average:	**2.9×10^5**

* Compound **4SF** was described previously,[4] but its affinity for chloride in $CHCl_3$ was not reported.

Measurement of affinities to $Bu_4N^+Cl^-$ in DMSO-d_6/H_2O (200:1) and $CDCl_3$ through ^1H NMR titrations

Binding constants to chloride were also assessed using ^1H NMR titrations against n-$Bu_4N^+Cl^-$ in DMSO-d_6/H_2O (200:1). The hygroscopic guest n-$Bu_4N^+Cl^-$ and the host compounds were dried under high vacuum to remove residual solvents or water prior to solution preparation. The concentration of the host was around 1 mM in all titrations; the concentration of guest and the volumes of the aliquots of guest solution added to the host solution were varied over the experiments. The guest solutions contained the same concentrations of host as the starting host solution [*i.e.*, n-$Bu_4N^+Cl^-$ was dissolved in a solution of ~1 mM host in DMSO-d_6/H_2O (200:1)], so that the concentration of host did not decrease over the course of the experiment. All ^1H NMR titration binding studies were performed using a Varian 500b NMR spectrometer at 298 K.

The shift of both NH signals in DMSO was fitted initially to 1:1 binding model using a least-squares fitting procedure in a custom-made Excel spreadsheet. The first 10-12 data points gave a reasonable fit to a 1:1 binding model, but the NMR signals continued to move upon addition of more chloride as is indicative for 1:2 binding. HypNMR2008 software (http://www.hyperquad.co.uk/)[5] was therefore used to fit the data to a 1:1 + 1:2 binding model. Firstly, both NH signals were fitted to a 1:1 model, then a second binding event of guest to the host-guest complex was introduced to the model, and the fit was refined. The binding constants obtained from this refined fit are reported in Table 1 and the fits to the most downfield NH signal are shown in Figures S7, S9, S11, S13, and S15.

The binding constant of **6SP** to chloride in $CDCl_3$ was determined in a similar manner; the host was dissolved in deacidified $CDCl_3$ to give a 0.1 mM solution. The guest solution was prepared by dissolving n-$Bu_4N^+Cl^-$ in 1 mL of the 0.1 mM host solution. The NH signals were hard to follow due to significant broadening and the aromatic signals overlapped with the solvent signal, so instead the signals from the ethyl groups (2.62 and 1.07 ppm.) were plotted and found to fit well to a 1:1 binding model (see Figure S17).[1]

[1] Attempts to roughly plot the shift of the NH signals of **6SP** in $CDCl_3$ gave curves nearly identical to those of the more accurately determined shifts of the ethyl signals. The curvature found when plotting the small shifts of the CH_2 signals of **6SF2** in DMSO was not significantly different from the curves found for the NH signals of **6SF2**. This justifies following different signals in different solvents.

^{1}H NMR titration of **6SP** with $Bu_4N^+Cl^-$ in DMSO-d_6/H_2O (200:1)

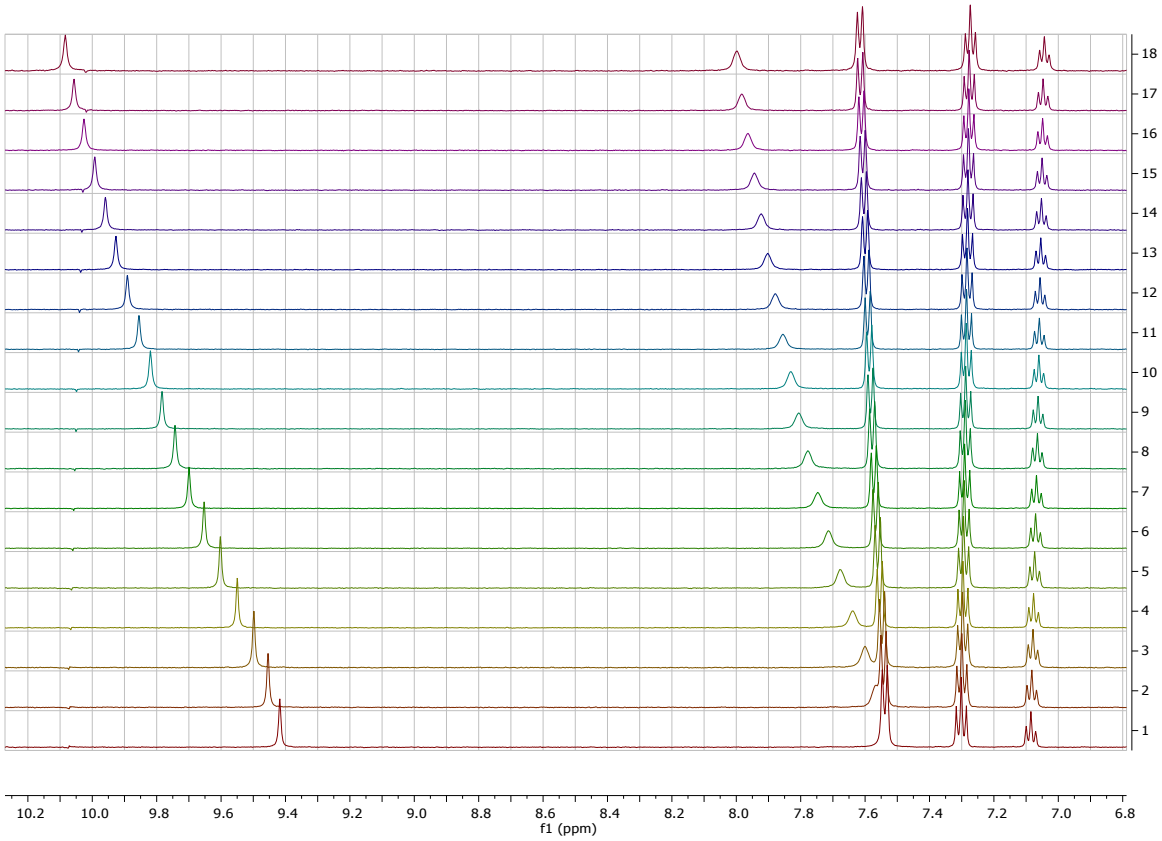

Figure S6. Downfield region of the ^{1}H NMR spectra from the titration of tetrabutylammonium chloride into **6SP** in DMSO-d_6/H_2O (200:1) at 298 K.

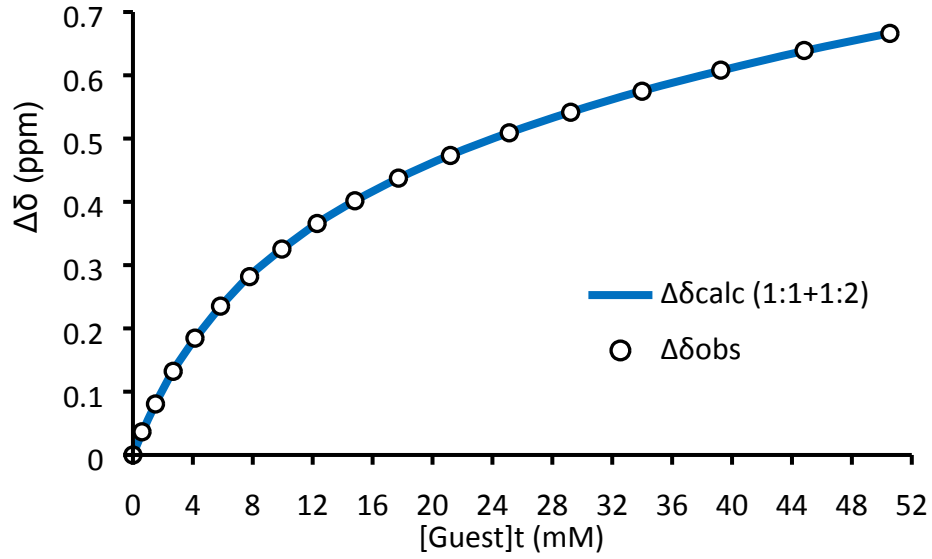

Figure S7. Graph showing observed data points (NH, starting at 9.42 ppm) and calculated fitting from the above titration of **6SP** with tetrabutylammonium chloride.

^{1}H NMR titration of **6SN** with $Bu_4N^+Cl^-$ in DMSO-d_6/H_2O (200:1)

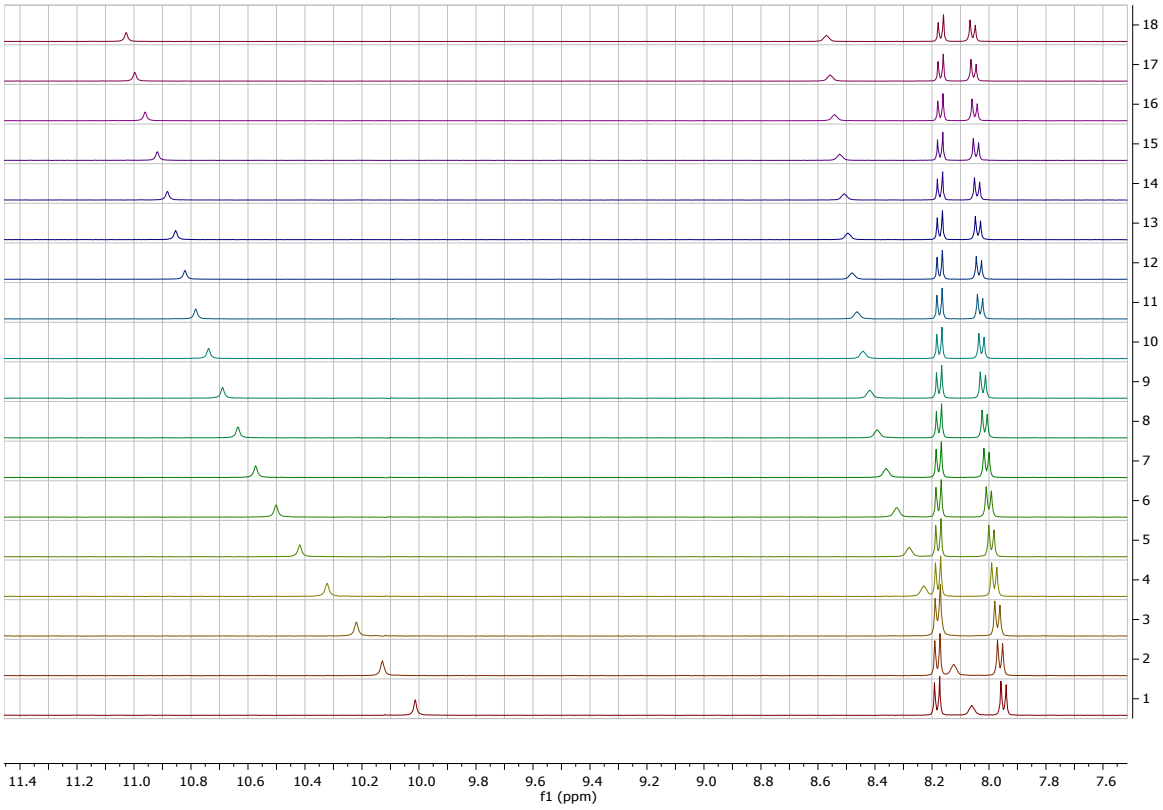

Figure S8. Downfield region of the ^{1}H NMR spectra from the titration of tetrabutylammonium chloride into **6SN** in DMSO-d_6/H_2O (200:1) at 298 K.

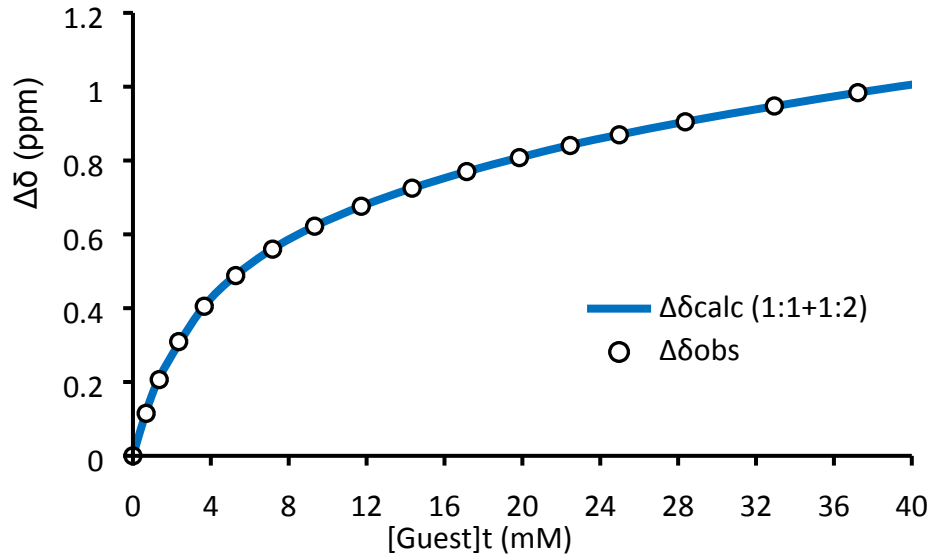

Figure S9. Graph showing observed data points (NH, starting at 10.01 ppm) and calculated fitting from the above titration of **6SN** with tetrabutylammonium chloride.

^{1}H NMR titration of **6SF** with $Bu_4N^+Cl^-$ in DMSO-d_6/H_2O (200:1)

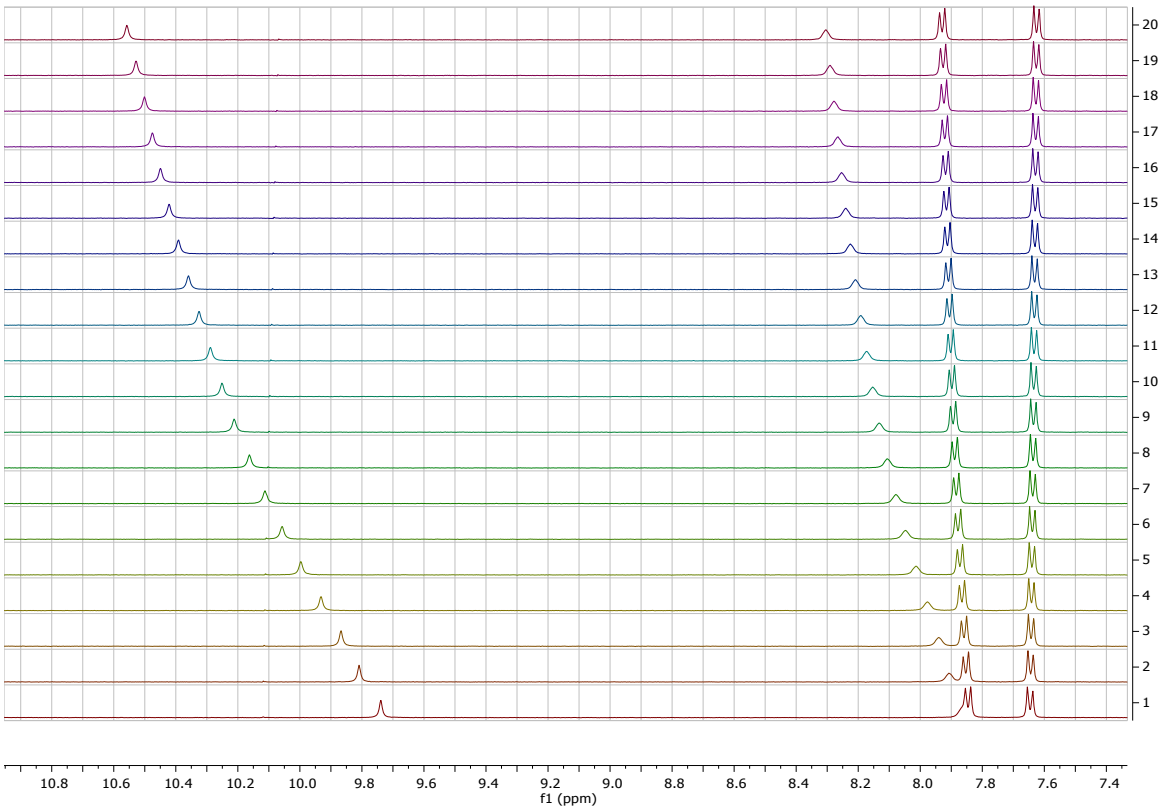

Figure S10. Downfield region of the ^{1}H NMR spectra from the titration of tetrabutylammonium chloride into **6SF** in DMSO-d_6/H_2O (200:1) at 298 K.

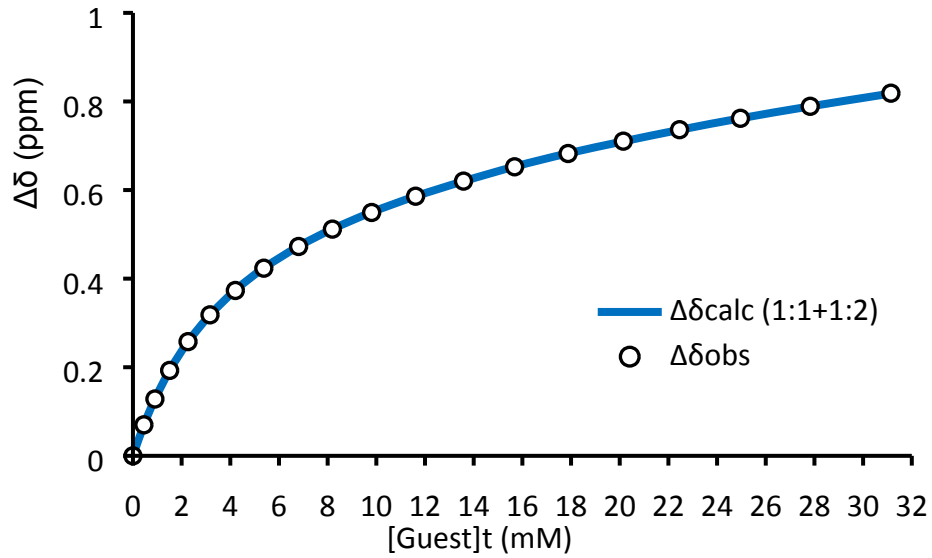

Figure S11. Graph showing observed data points (NH, starting at 9.74 ppm) and calculated fitting from the above titration of **6SF** with tetrabutylammonium chloride.

^{1}H NMR titration of **6SF2** with $Bu_4N^+Cl^-$ in DMSO-d_6/H_2O (200:1)

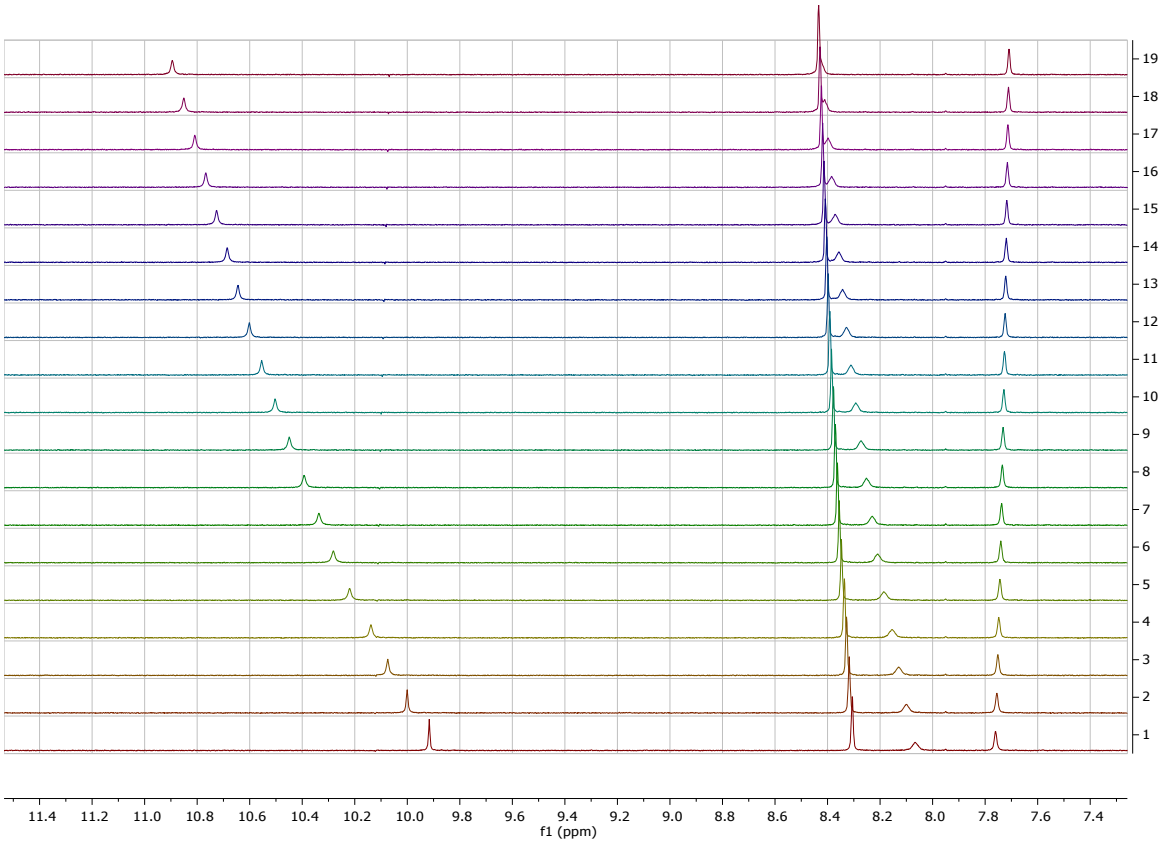

Figure S12. Downfield region of the ^{1}H NMR spectra from the titration of tetrabutylammonium chloride into **6SF2** in DMSO-d_6/H_2O (200:1) at 298 K.

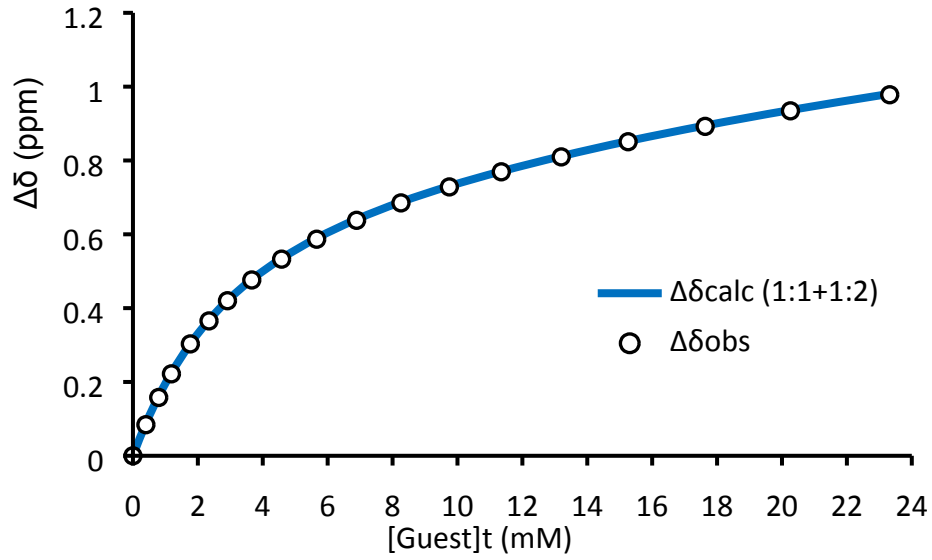

Figure S13. Graph showing observed data points (NH, starting at 9.92 ppm) and calculated fitting from the above titration of **6SF2** with tetrabutylammonium chloride.

^{1}H NMR titration of **6OF2** with $Bu_4N^+Cl^-$ in DMSO-d_6/H_2O (200:1)

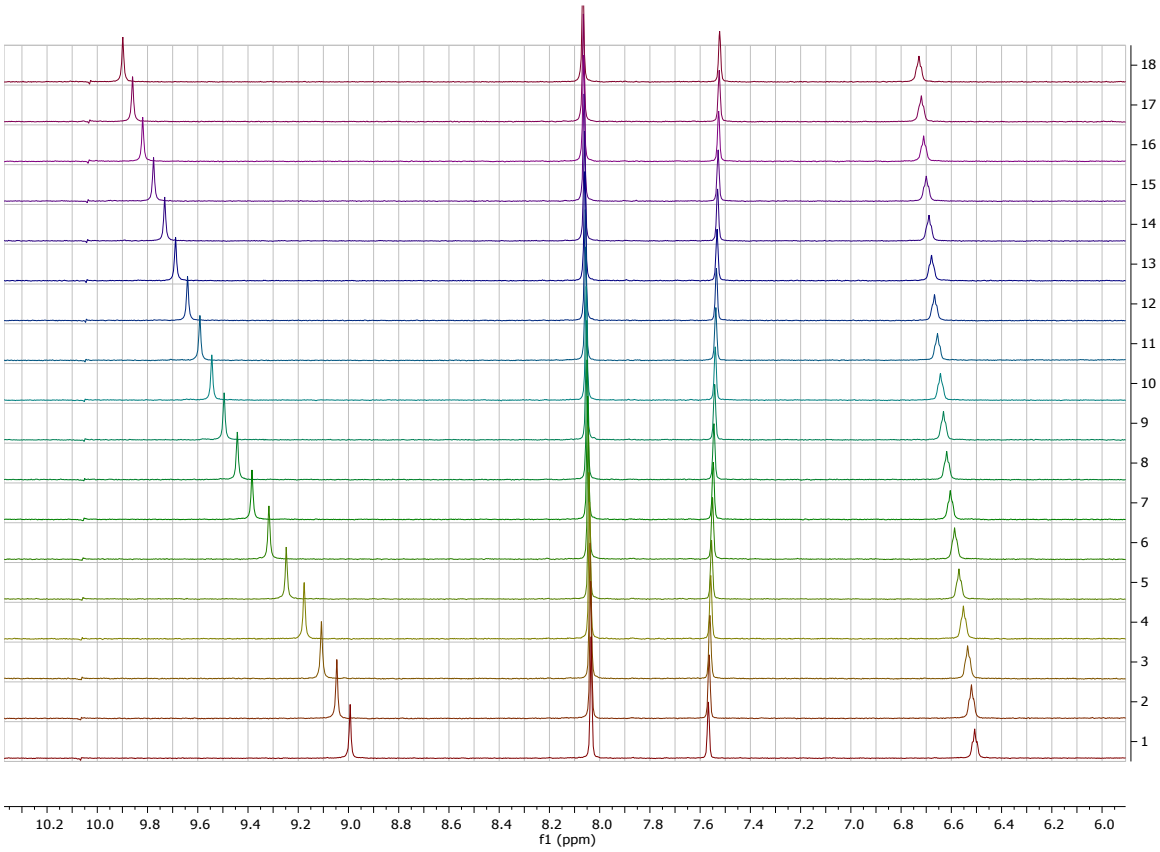

Figure S14. Downfield region of the ^{1}H NMR spectra from the titration of tetrabutylammonium chloride into **6OF2** in DMSO-d_6/H_2O (200:1) at 298 K.

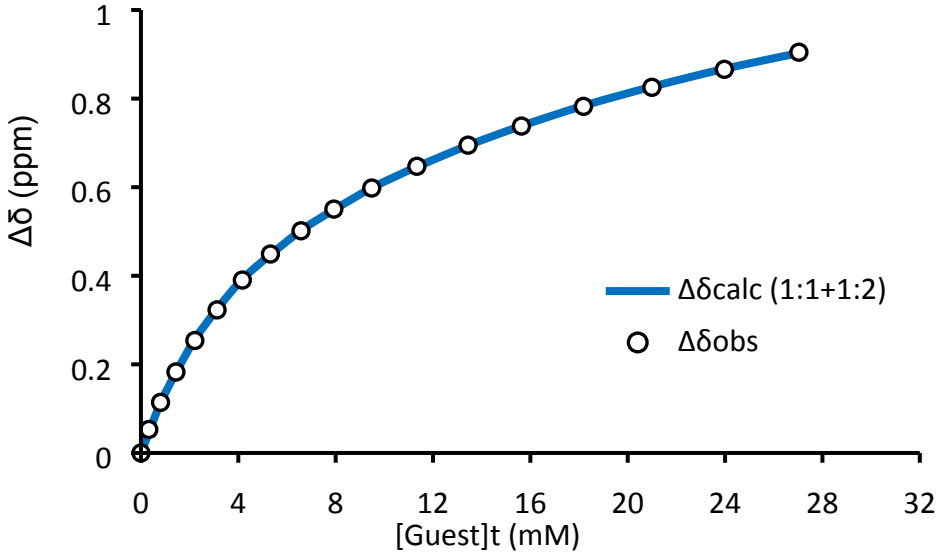

Figure S15. Graph showing observed data points (NH, starting at 8.99 ppm) and calculated fitting from the above titration of **6OF2** with tetrabutylammonium chloride.

^{1}H NMR titration of **6SP** with $Bu_4N^+Cl^-$ in $CDCl_3$

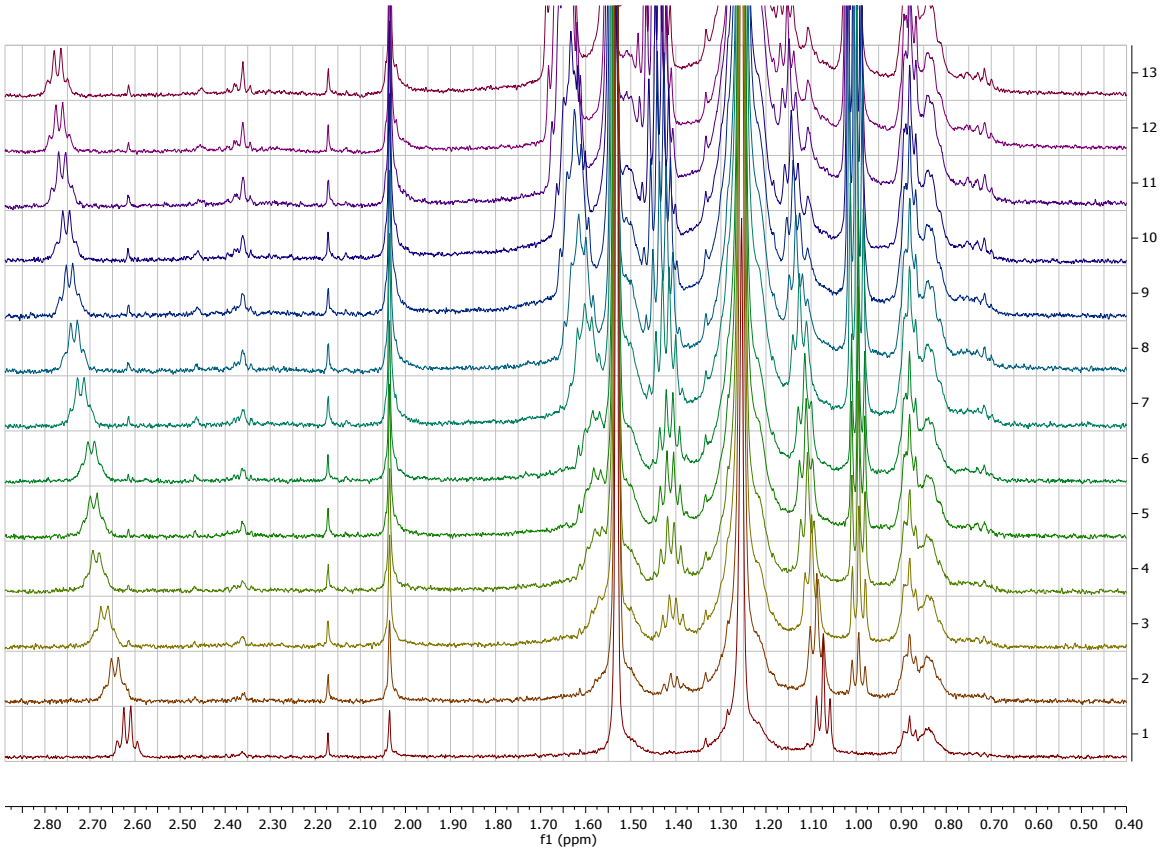

Figure S16. Upfield region of the ^{1}H NMR spectra from the titration of tetrabutylammonium chloride into **6SP** in deacidified $CDCl_3$.

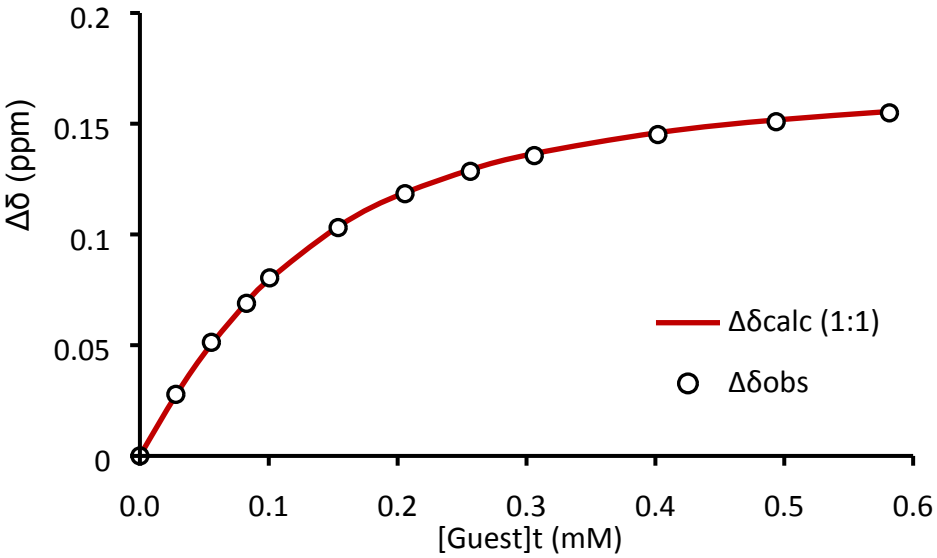

Figure S17. Graph showing observed data points (CH_2CH_3, starting at 2.63 ppm) and calculated fitting from the above titration of **6SP** with tetrabutylammonium chloride.

3. Transport measurements

General procedure for transport measurements

1-Palmitoyl-2-oleoyl-*sn*-glycero-3-phosphocholine (POPC) was obtained from Avanti® Polar Lipids, Inc. An extrusion apparatus and 200 nm polycarbonate membranes were obtained from GC Technology Ltd. All lipid and transporter solutions were prepared using chloroform that had been deacidified by passage through a flash chromatography column containing basic alumina and all aqueous solutions were prepared using deionised water that had been passed through a Millipore filtration system.

POPC and cholesterol solutions (~10 mM) in deacidified chloroform were combined with a solution of transporter in methanol (or in a mixture of methanol and deacidified chloroform) in a 5 mL round bottom flask. Volumes of the aliquots were calculated from the concentrations of the lipid solution to obtain a POPC to cholesterol ratio of 7:3 (for instance by combining 4.20 µmol POPC and 1.80 µmol cholesterol). The ratio of transporter to lipid (POPC + cholesterol) was varied from 1:2500 to 1:25000, as specified in the experiments. The solvents from the lipid/receptor mixture were evaporated under a stream of N_2 and the lipid film was dried under high vacuum for 1 h. The residue was hydrated with 500 µL of an aqueous solution of 10,10'-dimethyl-9,9'-biacridinium nitrate (lucigenin, 0.8 mM) and $NaNO_3$ (225 mM), sonicated for 30 s and stirred for 1 h to give heterogeneous vesicles. Multilamellar vesicles were disrupted by 10 freeze-thaw cycles and then the solution was diluted to 1 mL (by adding 0.5 mL of 225 mM $NaNO_3$) and carefully extruded (29 times) through a polycarbonate membrane (200 nm pore size). The external lucigenin was removed by passing the solution though a size exclusion column (containing ~2 g Sephadex 50G, eluted with 225 mM $NaNO_3$). The collected vesicles were further diluted with $NaNO_3$ solution (225 mM) to obtain a vesicle solution with 0.4 mM lipid concentration. 3.00 mL of this vesicle solution was placed in a quartz cuvette with a small stir bar and the fluorescence intensity (excitation at 450 nm, emission at 535 nm) was measured over time at 25 ˚C, using a PerkinElmer LS45 fluorescence spectrometer. 75 µL of aqueous NaCl (1.0 M in 225 mM $NaNO_3$, to give an overall exterior chloride concentration of 25 mM Cl^-) was added ~30 seconds after the start of the measurement and the fluorescence intensity was measured for another 14 minutes.

Fluorescence data were collected for at least four of these runs. The plateau (before addition of chloride) and the vertical drop (the first 1-2.5 seconds after chloride addition, due to quenching of external lucigenin) were removed. Next the data were normalized: all fluorescence values (F) were divided by the fluorescence value before addition of chloride (F_0). These normalized traces were averaged and are plotted in Figure 3 of the main paper.

Quantification of transport rates based on fluorescence data

As detailed in our previous publication (Ref. 6), the inverse of the normalized fluorescence traces: $\left(\frac{F}{F_0}\right)^{-1} = \left(\frac{F_0}{F}\right)$ is directly proportional to concentration of chloride inside the vesicles, according to the Stern-Volmer equation. Therefore F_0/F was used in the following calculations of transport rates. Data analysis, including curve fitting, was performed using Origin 9.

Half-lives $t_{½}$: To obtain decay half-lives the F_0/F curves (0-500 s) were then fitted to a single exponential decay function:

$$\frac{F_0}{F} = y - ae^{-bt}$$

and the half-life $t_{½}$ was calculated from fit parameter 'b' using: $t_{½} = \frac{ln(2)}{b}$

Initial rates (I): To obtain initial rates, the F_0/F curves were also fitted to a double exponential decay function:

$$\frac{F_0}{F} = y - ae^{-bt} - ce^{-dt}$$

Differentiating this gives $\frac{d(\frac{F_0}{F})}{dt} = abe^{-bt} + cde^{-dt}$

and substituting $t = 0$ gives the following equation for initial rate (I): $I = ab + cd$

Specific Initial Rate [I]: To obtain a quantitative measure for the performance of anion transporters independent of transporter:lipid ratio, the initial rates were divided by the transporter:lipid ratio. The obtained value was then averaged over the experiments at different ratios (*i.e.*, 1:2500 and 1:25000) to obtain the Specific Initial Rate [I], as reported in Table 1 of the main text. A more detailed study of **6SF2** (see below) confirmed the linear dependence between transport rates and transporter loading.

Comparison of **6SF2** with previously reported highly active chloride transporters

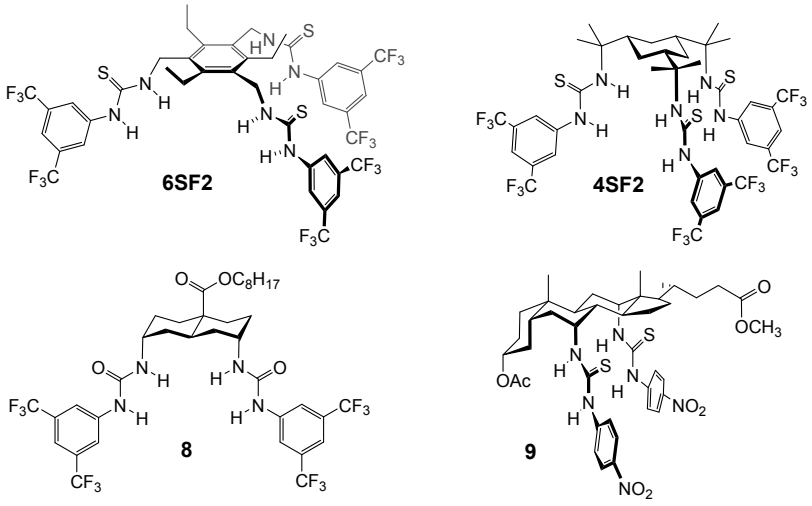

In the graph below we show how **6SF2** (blue) gives very similar curvature (and thus similar rates of anion transport) compared to three other potent anion carriers reported by our group.

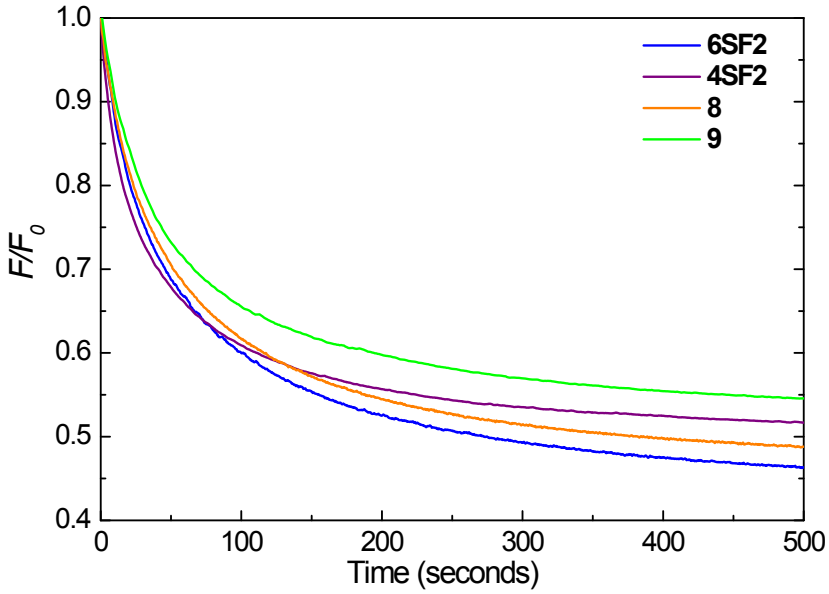

Figure S18. Graph of transport by **6SF2** (preincorporated in POPC/cholesterol 7:3 vesicles) compared to that of highly active transporters that have been previously reported by our group: **4SF2**[4], **8**[7] and **9**[8]. All transporters are preincorporated at a transporter to lipid ratio of 1:25000.

Transport by **6SF2** at various loadings

The specific initial rates [*I*], reported in Table 1, are only meaningful if transport rates vary linearly with transporter loadings. To confirm that this is the case, anion transport by **6SF2** was studied at an additional three transporter:lipid ratios (1:10000, 1:50000, and 1:250000) following the methodology described above. The full set of fluorescence decay traces is shown in Figure S19.

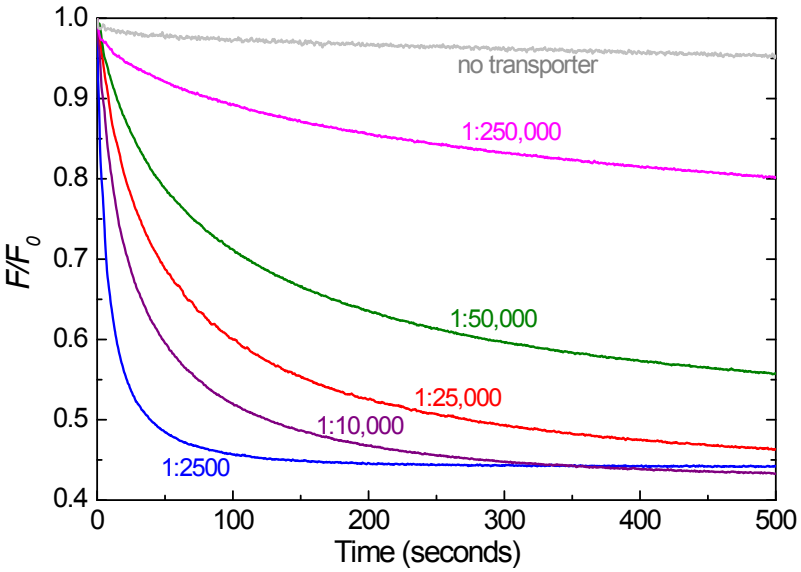

Figure S19. Chloride/nitrate exchange by **6SF2** in 200 nm POPC/cholesterol (7:3) vesicles, as followed by the lucigenin method at various transporter:lipid ratios as indicated in the graph.

The concentration-dependence data in Figure S19 were analysed by two different methods. Firstly, the initial rates of transport were plotted as a function of the transporter concentration in the vesicles (Figure S20).

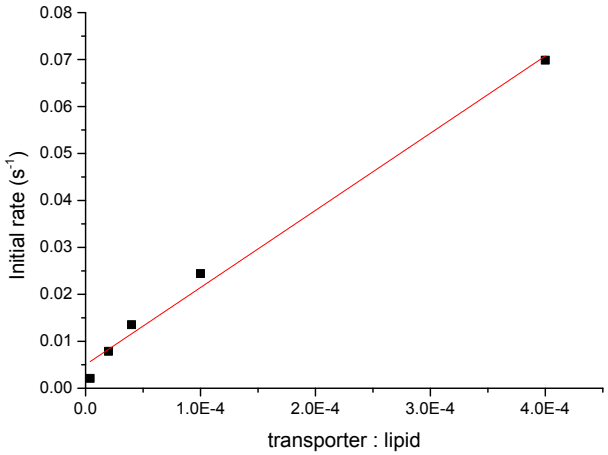

Figure S20. Plot of the initial rates of chloride transport versus the **6SF2**:lipid ratio (black squares) and a linear fit of the data (red line).

In agreement with our previously reported results for cholapod and decalin based thioureas,[6] the initial rates increased nearly linearly with the concentration. As well as confirming the validity of [*I*] as a measure of transport activity, this result suggests that monomeric **6SF2** is responsible for the observed anion transport, as opposed to the dimeric species observed in the crystal structure (Fig. 5). If transport were performed by the dimer of **6SF2**, a quadratic increase of initial rate with transporter concentration would have been expected.

Additionally, the data were analysed using the Hill equation. For this analysis we used the F_o/F values at 270 s as measure for the chloride concentration inside the vesicles at that point in time and fitted these with the 'Hill1' equation in Origin 9.0.0 (Figure S21). This fit gave a Hill coefficient *n* of 1.4. This is more than the value of $n = 1$ expected for a carrier acting as a monomer, but not clearly indicating transport by the dimeric species either. We should note that Hill coefficients > 1 are not unprecedented for compounds which are considered to be monomeric anion carriers.[9] Taking into account both methods of data analysis, we consider the nearly linear (and definitely not quadratic) plot of the initial rate vs. loading to be a clear indication that **6SF2** is acting as a monomeric carrier.

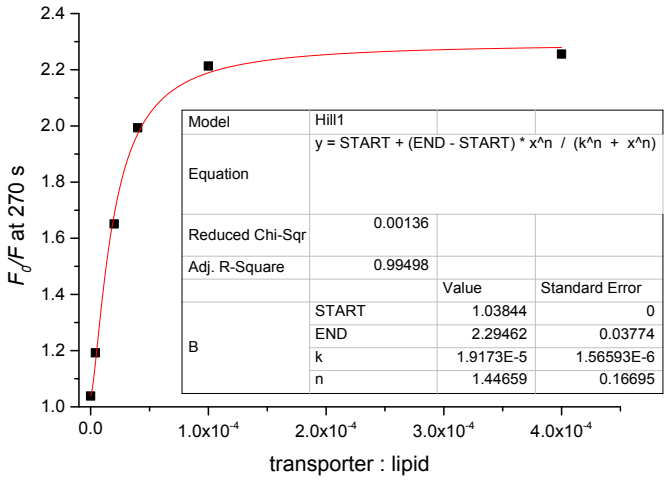

Figure S21. Plot of the chloride concentration inside the vesicles 270 s (given by F_0/F) after the addition of NaCl versus the **6SF2**:lipid ratio (black squares) and a fit of these data to the Hill equation (red line). The inset gives the equation used for the fit and the resulting parameters. The EC_{50} value is represented by parameter *k* and the Hill coefficient by parameter *n*.

The Hill analysis also gives an $EC_{50,\ 270s}$ value (*i.e.*, the concentration required to obtain half of the maximum effect, in our case the transporter:lipid ratio required to give a chloride concentration of 12.5 mM inside the vesicles), as represented by parameter *k* in the equation and fit. We found an $EC_{50,\ 270s}$ of 1.9×10^{-5} (or 0.0019 mol%), corresponding to a **6SF2** to lipid ratio of 1:52,000. Though $EC_{50,\ 270s}$ values for anion carriers reported by other groups are generally obtained from different assays and under different conditions, so that direct comparisons cannot be made, it is interesting to note that this value is among the lowest reported in the literature. In comparison, values down to 0.0044 mol% are quoted for tren-based systems,[9] while the lowest reported figure for Cl^-/NO_3^- exchange is 0.0015 mol%[10].

Transport by **6SF2** in DPPC vesicles

To test if **6SF2** transports anions as a mobile carrier, transport experiments were repeated using vesicles prepared from dipalmitoylphosphatidylcholine (DPPC). This lipid undergoes a transition between fluid and gel phases at 41 °C.[11] If transport studies are performed on either side of this temperature, the performance of an anion carrier should be greatly affected by the transition while that of a channel should not.[11,12] The method may be unreliable if the transporter is liable to ejection from the membrane at the lower temperatures,[13] but in the case of hydrophobic molecules such as **6SF2** this should not apply. For further discussion of this issue, see ref [4].

A solution of 548 μL of 1,2-dipalmitoyl-*sn*-glycero-3-phosphocholine (DPPC, 10.59 mM, 6.0 μmol) in deacidified chloroform was mixed with 85.7 μL of transporter **6SF2** (28.00 μM, 2.4 nmol) in methanol to reach a transporter to lipid ratio of 1:2500. The solvents were evaporated by a slow stream of nitrogen, followed by drying under vacuum for at least an hour. Then 500 μL of an aqueous solution of 0.8 mM *N,N′*-Dimethyl-9,9′-biacridinium dinitrate (Lucigenin) in 225 mM $NaNO_3$ was added, and the suspension was sonicated for 10 min at 59 °C. The suspension was then stirred for one hour at 50 °C. The suspension was frozen and thawed 10 times with liquid N_2 and lukewarm water, respectively, in order to break up multilamellar vesicles. The vesicle solution was extruded through a polycarbonate membrane with 200 nm pores 29 times, while the temperature was kept around 50 °C, in order to give a mean diameter of vesicles of ~200 nm. The vesicles were cooled to room temperature and the external lucigenin was removed by passing the solution though a size exclusion column (containing ~2 g Sephadex 50G, eluted with 225 mM $NaNO_3$). The collected vesicles were further diluted with $NaNO_3$ solution (225 mM) to obtain a vesicle solution with 0.4 mM lipid concentration.

3.00 mL of this vesicle solution was placed in a quartz cuvette with a small stir bar and the fluorescence intensity (excitation at 450 nm, emission at 535 nm) was measured over time at 25 ˚C (2 runs) and at 45 ˚C (2 runs), using a PerkinElmer LS45 fluorescence spectrometer. 75 μL of aqueous NaCl (1.0 M in 225 mM $NaNO_3$, to give an overall exterior chloride concentration of 25 mM Cl^-) was added ~30 seconds after the start of the measurement and the fluorescence intensity was measured for another 14 minutes. Data were processed as before and the results are shown below in Figure S22.

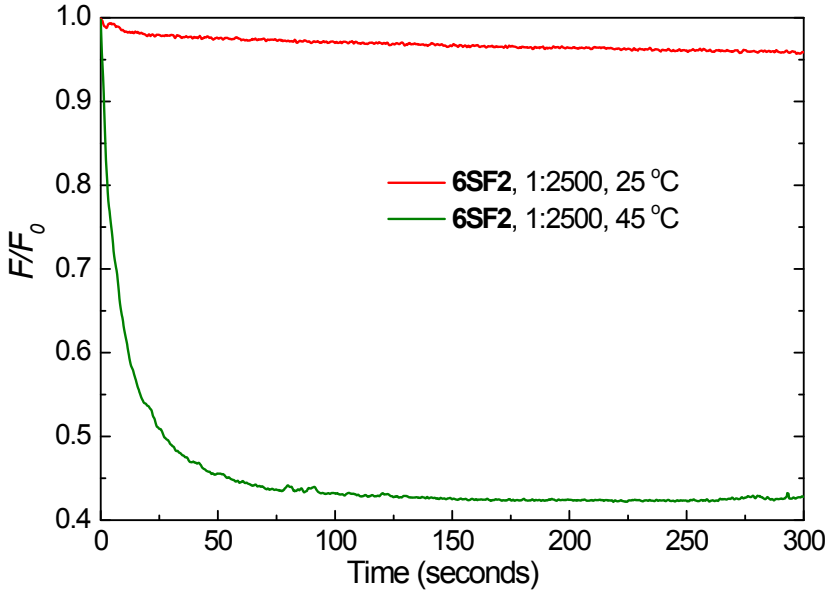

Figure S22. Graph of transport by **6SF2** preincorporated in vesicles composed of DPPC at a transporter to lipid ratio of 1:2500 at 25 °C (gel phase) and at 45 °C (liquid crystalline phase).

Figure S22 shows that **6SF2** does transport in DPPC vesicles at 45 °C (liquid crystalline phase), but not at 25 °C (gel phase), indicating a mobile carrier mechanism.

4. Molecular modelling of 6OP

Tris-urea **6OP**

Initial modelling of **6OP** was performed using Maestro 9.7/MacroModel 10.3 (Schrödinger Inc.) employing the OPLS_2005 force-field. A Monte Carlo Molecular Mechanics (MCMM) conformational search, in which all acyclic bonds were allowed to rotate, yielded a conformation with convergent NH groups similar to that shown in Figure 2a. This conformation was then energy-minimised by *ab initio* calculations (Hartree-Fock, 6-31+G* basis set) using Spartan '06 to give the structure in Fig. 2a.

Chloride complex of **6OP**

The complex **6OP**.Cl^- was subjected to an MCMM search as described above, yielding a conformation with 4 NH···Cl^- hydrogen bonds and an *E*-NHCO unit as the global minimum. *Ab initio* energy minimisation in Spartan, as above, then yielded the conformation in Fig. 2c. In a separate calculation, Spartan was used to generate a C_{3v} structure with 6 NH···Cl^- hydrogen bonds. This was then energy-minimised using *ab initio* methodology, retaining the C_{3v} symmetry, to give the structure in Fig. 2b.

5. X-ray crystal structure of 6SF2.TMACl

Single crystal X-ray data for **6SF2.TMACl** were measured at 123 K with Agilent Super-Nova dual source wavelength diffractometer with an Atlas CCD detector using multilayer optics monochromatized Cu- Kα (λ = 1.54184 Å) radiation. The data collection and reduction for **6SF2.TMACl** were performed using the program *CrysAlisPro*,[14] and the intensities were corrected for absorption using gaussian face index absorption correction method.[14] The structure was solved with direct methods (*SHELXS*[15]) and refined by full-matrix least squares on F^2 using *OLEX2*,[16] which utilizes the *SHELXL*-2013 module.[15] No attempt was made to locate the hydrogens and some spurious electron residual peaks were masked from the difference Fourier maps.

Table S2. Crystal data and X-ray experimental details for **6SF2.TMACl**.

Complex	**6SF2.TMACl**
Empirical formula	$C_{88}H_{88}Cl_2F_{36}N_{13}O_2S_6$
Formula weight	2306.97
Temperature (K)	123.0
Crystal system	Monoclinic
Space group	*C2/c*
Unit cell dimensions: a (Å)	20.3759(13)
b (Å)	35.024(4)
c (Å)	16.9047(10)
α (°)	90
β (°)	98.951(6)
γ (°)	90
Volume / Å^3	11917.2(17)
Z	4
Density (calculated) mg/m^3	1.286
Absorption Coefficient mm^{-1}	2.385
F(000)	4708
Crystal size (mm^3)	0.19 x 0.12 x 0.05
θ range for data collection (°)	3.65 to 76.75
Reflections collected [R(int)]	21625 [0.0787]
Observed reflections [I>2σ(I)]	4589
Data completeness (%)	95.58
Data/ restraints/ parameters	12014/0/689
Goodness-of-fit on F^2	1.019
Final R_1 indices [I>2σ(I)]	R_1 = 0.1378, wR_2 = 0.3462
Final R indices [all data]	R_1 = 0.1993, wR_2 = 0.4106
Largest diff. peak/hole (e.Å^{-3})	0.586/ -0.673

References

[1] A. B. Pangborn, M. A. Giardello, R. H. Grubbs, R. K. Rosen and F. J. Timmers, *Organometallics*, 1996, **15**, 1518–1520.

[2] J. P. Clare, A. J. Ayling, J.-B. Joos, A. L. Sisson, G. Magro, M. N. Pérez-Payán, T. N. Lambert, R. Shukla, B. D. Smith and A. P. Davis, *J. Am. Chem. Soc.*, 2005, **127**, 10739–10746.

[3] A. J. Ayling, S. Broderick, J. P. Clare, A. P. Davis, M. N. Pérez-Payán, M. Lahtinen, M. J. Nissinen and K. Rissanen, *Chem. Eur. J.*, 2002, **8**, 2197–2203.

[4] J. A. Cooper, S. T. G. Street and A. P. Davis, *Angew. Chem. Int. Ed.*, 2014, **53**, 5609–5613.

[5] C. Frassineti, L. Alderighi, P. Gans, A. Sabatini, A. Vacca and S. Ghelli, *Anal Bioanal Chem*, 2003, **376**, 1041–1052.

[6] H. Valkenier, L. W. Judd, H. Li, S. Hussain, D. N. Sheppard and A. P. Davis, *J. Am. Chem. Soc.*, 2014, **136**, 12507–12512.

[7] S. Hussain, P. R. Brotherhood, L. W. Judd and A. P. Davis, *J. Am. Chem. Soc.*, 2011, **133**, 1614–1617.

[8] B. A. McNally, A. V. Koulov, T. N. Lambert, B. D. Smith, J.-B. Joos, A. L. Sisson, J. P. Clare, V. Sgarlata, L. W. Judd, G. Magro and A. P. Davis, *Chem. Eur. J.*, 2008, **14**, 9599–9606.

[9] N. Busschaert, M. Wenzel, M. E. Light, P. Iglesias-Hernández, R. Pérez-Tomás and P. A. Gale, *J. Am. Chem. Soc.*, 2011, **133**, 14136–14148.

[10] L. E. Karagiannidis, C. J. E. Haynes, K. J. Holder, I. L. Kirby, S. J. Moore, N. J. Wells and P. A. Gale, *Chem. Commun.*, 2014, **50**, 12050–12053.

[11] M. J. Pregel, L. Jullien, J. Canceill, L. Lacombe and J. M. Lehn, *J. Chem. Soc., Perkin Trans. 2*, 1995, 417-426.

[12] G. Deng, T. Dewa and S. L. Regen, *J. Am. Chem. Soc.*, 1996, **118**, 8975-8976.

[13] S. Otto, M. Osifchin and S. L. Regen, *J. Am. Chem. Soc.*, 1999, **121**, 10440-10441.

[14] *CrysAlisPro* 2012, Agilent Technologies. Version 1.171.36.35.

[15] Sheldrick, G. M. *Acta Cryst. A* 2008, **64**, 112–122.

[16] Dolomanov, O. V.; Bourhis, L. J.; Gildea, R. J.; Howard, J. A. K. and Puschmann, H. *J. Appl. Cryst.* **2009**, *42*, 339–341.